A mechanism for induction of a hypoxic response by vaccinia virus

Michela Mazzon[a,b,1], Nicholas E. Peters[b,1], Christoph Loenarz[c,1], Ewelina M. Krysztofinska[b], Stuart W. J. Ember[a,b], Brian J. Ferguson[a,b], and Geoffrey L. Smith[a,b,2]

[a]Department of Pathology, University of Cambridge, Cambridge CB2 1QP, United Kingdom; [b]Department of Virology, Faculty of Medicine, Imperial College London, St. Mary's Campus, London W2 1PG, United Kingdom; and [c]Chemistry Research Laboratory, Department of Chemistry, University of Oxford, Oxford OX1 3TA, United Kingdom

Edited by Ruslan Medzhitov, Yale University School of Medicine, New Haven, CT, and approved June 10, 2013 (received for review February 5, 2013)

Viruses have evolved sophisticated strategies to exploit host cell function for their benefit. Here we show that under physiologically normal oxygen levels (normoxia) vaccinia virus (VACV) infection leads to a rapid stabilization of hypoxia-inducible factor (HIF)-1α, its translocation into the nucleus and the activation of HIF-responsive genes, such as vascular endothelial growth factor (VEGF), glucose transporter-1, and pyruvate dehydrogenase kinase-1. HIF-1α stabilization is mediated by VACV protein C16 that binds the human oxygen sensing enzyme prolyl-hydroxylase domain containing protein (PHD)2 and thereby inhibits PHD2-dependent hydroxylation of HIF-1α. The binding between C16 and PHD2 is direct and specific, and ectopic expression of C16 alone induces transcription of HIF-1α responsive genes. Conversely, a VACV strain lacking the gene for C16, *C16L*, is unable to induce HIF-1α stabilization. Interestingly, the N-terminal region of C16 is predicted to have a PHD2-like structural fold but lacks the catalytic active site residues of PHDs. The induction of a hypoxic response by VACV is reminiscent of the biochemical consequences of solid tumor formation, and illustrates a poxvirus strategy for manipulation of cellular gene expression and biochemistry.

Orthopoxvirus | variola virus | Warburg effect | glucose metabolism

Vaccinia virus (VACV) is the live vaccine used against smallpox, an extinct human disease caused by variola virus (VARV) (1). VACV and VARV belong to the *Orthopoxvirus* genus of the *Poxviridae*, and each have large dsDNA genomes and replicate in the cell cytoplasm (2). VACV can be engineered to express foreign genes and these recombinant viruses have potential as live vaccines against other diseases (3) and are useful laboratory tools, for instance in identifying the target antigens of CD8+ cytotoxic T lymphocytes (4, 5). VACV encodes many genes that are nonessential for virus replication but are important in vivo for defense against the host innate immune system, such as the VACV steroid biosynthetic enzyme 3-β-hydroxysteroid dehydrogenase (6, 7), or for modulation of host cell biochemistry, such as the VACV enzymes thymidine kinase (8), thymidylate kinase (9), and ribonuceotide reductase (10).

VACV strain Western Reserve (WR) gene *C16L* encodes a 37-kDa intracellular protein that contributes to virulence by an unknown mechanism (11). C16 is nonessential for VACV replication, yet orthologs of C16 are conserved in several poxviruses, suggesting an important function (11). VACV also encodes a related protein, C4, with 43% amino acid identity to C16 and that inhibits activation of NF-κB (12).

Here a direct interaction is shown between the N-terminal region of C16 and the human oxygen sensor prolyl-hydroxylase domain containing protein (PHD)2. During normoxia, PHD2 is the major enzyme that hydroxylates hypoxia-inducible factor (HIF)-1α on either of two proline residues within the oxygen-dependent degradation domain (ODD), P402 and P564 (13, 14). After hydroxylation, HIF-1α is ubiquitinated by the von Hippel–Lindau E3-ubiquitin ligase and then degraded by the proteasome. In contrast, under low oxygen levels (hypoxia), PHD2 is inactive and so HIF-1α is not hydroxylated, remains stable and translocates to the nucleus where it induces transcription of many genes involved in adaptation to hypoxia, including those promoting angiogenesis, glucose metabolism, and cell survival (reviewed in refs. 15 and 16). Although other substrates have been suggested for PHD2, HIF-1α remains the best studied target, and oxygen sensing is considered the main function of this hydroxylase (17–19).

Here we show that by binding to PHD2, C16 inhibits PHD2-mediated hydroxylation of HIF-1α leading to HIF-1α stabilization early after VACV infection and to the up-regulation of HIF-responsive genes. Thereby, VACV creates a hypoxic response under normoxic conditions that mimics the situation in solid tumors. Intriguingly, the inhibition of PHD2 is mediated via the N-terminal region of C16 that is predicted to adopt a PHD2-like fold but lacks the amino acid residues needed for catalytic activity.

Results

C16 Binds to Human PHD2. To investigate how protein C16 contributes to VACV virulence, binding partners of C16 were sought using C16 fused at the C terminus with STREP and FLAG tags (C16-TAP). A HEK293T cell line expressing an inducible C16-TAP was created and C16-TAP was isolated by tandem affinity purification (TAP) (20). SDS/PAGE showed that C16 copurified with a 50-kDa protein that was not seen from the same uninduced cell line, or from a cell line expressing the TAP-tag alone (Fig. S1). Liquid chromatography-mass spectrometry (LC-MS) unambiguously identified the 50-kDa protein as human PHD2 (egg-laying 9 homolog 1), which has a predicted mass of 46 kDa.

The C16–PHD2 interaction was tested by immunoblotting after purification of C16-TAP expressed by transfection. Two other TAP-tagged VACV proteins, C6 (21, 22) and C4 (12) were analyzed in parallel. VACV C4-TAP was included because of its similarity with C16 (11, 12). C16 bound to endogenous PHD2 whereas C4 and C6 did not (Fig. 1*A*).

Two other human HIF-1α prolyl-hydroxylases are known, PHD1 and PHD3. Although PHD1-3 are involved in oxygen sensing, they are regulated differently, and may have different substrate specificities and HIF-independent functions (17, 19). To test whether C16 can also bind PHD1 or PHD3, C16-TAP affinity-purified samples were immunoblotted with specific Abs,

Author contributions: M.M., N.E.P., C.L., E.M.K., S.W.J.E., B.J.F., and G.L.S. designed research; M.M., N.E.P., C.L., E.M.K., S.W.J.E., and B.J.F. performed research; M.M., N.E.P., C.L., E.M.K., S.W.J.E., B.J.F., and G.L.S. analyzed data; and M.M., N.E.P., C.L., S.W.J.E., B.J.F., and G.L.S. wrote the paper.

The authors declare no conflict of interest.

This article is a PNAS Direct Submission.

Freely available online through the PNAS open access option.

[1]M.M., N.E.P., and C.L. contributed equally to this work.

[2]To whom correspondence should be addressed. E-mail: gls37@cam.ac.uk.

This article contains supporting information online at www.pnas.org/lookup/suppl/doi:10.1073/pnas.1302140110/-/DCSupplemental.

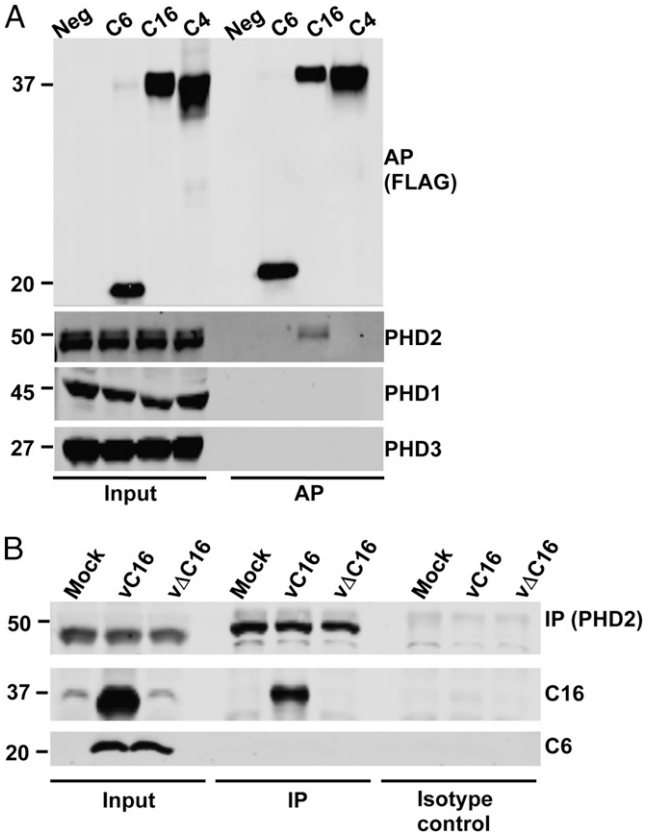

Fig. 1. VACV C16 protein binds to PHD2, but not to PHD1 or PHD3. (*A*) Lysates from HEK293T cells transfected with VACV C16-TAP, C4-TAP or C6-TAP, or untransfected (Neg) were affinity purified (AP) with streptavidin agarose. Proteins in whole cell lysates (Input) and in AP fractions were analyzed by SDS/PAGE and immunoblotting using Abs against FLAG, PHD1, PHD2, or PHD3. (*B*) PHD2 was immunoprecipitated (IP) from HEK293T cells infected with vC16 or vΔC16 at 10 pfu per cell for 2 h. Proteins in the whole cell lysates (Input) and the IP fractions were separated by SDS/PAGE and analyzed by immunoblotting using Abs against PHD2, C16 or C6. The positions of molecular mass markers are shown in kDa.

but only PHD2 purified with C16 (Fig. 1*A*). C16–PHD2 binding was also shown during VACV infection (vC16; ref. 11) where endogenous PHD2 coprecipitated with C16, but not C6 (Fig. 1*B*). The PHD2–C16 interaction was also confirmed by affinity purification of overexpressed PHD2 in the context of viral infection (Fig. S1*B*).

To test whether C16 binds PHD2 directly, C16 (Fig. S2 *A* and *B*) and PHD2 residues 181–426 ($PHD2_{181–426}$) were expressed and purified from *E. coli* and their binding was tested in vitro using size-exclusion chromatography. SDS/PAGE and immunoblot analysis of different size-exclusion chromatography fractions showed that, despite their different sizes, C16 and PHD2 coeluted (Fig. S2*C*). Together these results show that C16 binds PHD2 directly. Additionally, the C16–PHD2 interaction required only the C-terminal domain of PHD2 (residues 181–426), which contains the catalytic domain responsible for HIF-1α hydroxylation.

C16 Has a Predicted PHD2-Like Conformation. The potential 3D structure of C16 was studied by sequence-structure homology analysis using the PsiPred protein structure prediction server (http://bioinf.cs.ucl.ac.uk/psipred). The first 205 residues of C16 revealed strong similarity to prolyl-hydroxylases with those from *Shewanella baltica* and *Chlamydia reinhardtii* being most similar, and with more distant similarity to human PHD2. Alignment of $C16_{1–192}$ and human $PHD2_{227–426}$ indicated a low overall sequence similarity with some β-sheets (Fig. 2*A*), but using Modeler software (23) $C16_{1–192}$ mapped onto the known structure of PHD2 (24). Although the predicted secondary structure of C16 differs slightly from PHD2 in that it lacks the first two α-helices of PHD2, the double-stranded β-helix, the key structural feature of 2-oxoglutarate oxygenases including PHD2, is conserved in C16 (Fig. 2*B*).

Structural similarity between C16 and PHD2 is interesting because, although PHD2 crystallized as a homotrimer, it is not known to dimerize in solution (24). We therefore tested whether the N-terminal region of C16 is the domain required for binding PHD2. Lysates from HEK293T cells expressing either N-terminal $C16_{1–214}$ (ΔC-C16) or C-terminal $C16_{215–331}$ (Δ*N*-C16) were affinity purified, and binding of PHD2 was assessed by immunoblotting. Full-length C16 was included as control. $C16_{1–214}$ alone bound PHD2, whereas $C16_{215–331}$ did not. Therefore, the C16 N-terminal region with predicted PHD2-like conformation is also the region necessary for binding PHD2.

The C-terminal region of PHD2, which adopts the double-stranded β-helix fold, is responsible for the interaction with HIF-1α (25). Although this is predicted to be structurally conserved between C16 and PHD2, key catalytic residues of PHD2 (H313, D315, and H374) required to coordinate Fe(II) within the active site (24) are missing in C16, whereas the PHD2 residue R383, which coordinates 2-oxoglutarate (2OG), is conserved (Fig. 2*A*). Thus, the C16 N-terminal region might adopt a PHD2-like conformation, but it is unlikely to be catalytically active.

C16 Inhibits PHD2-Mediated Hydroxylation of HIF-1α and Induces HIF-1α Stabilization. PHD2 hydroxylates HIF-1α in normoxia, leading to HIF-1α degradation by the proteasome (18, 19). To test whether C16 inhibited PHD2 activity, recombinant $PHD2_{181–426}$ was coincubated with C16 and a HIF-1α fragment representing the CODD and HIF-1α hydroxylation was measured by MS (Fig. 3*A*). At C16 levels above equimolar to PHD2, but below equimolar to the HIF-1α substrate, C16 reduced HIF-1α CODD hydroxylation. These results are consistent with C16 binding to PHD2 and thereby hindering HIF-1α binding.

To investigate whether the inhibition of HIF-1α hydroxylation by C16 was specific to the HIF-1α domain targeted by PHD2, HIF-1α amino acids 395–413 and 556–574 representing the N-terminal oxygen-dependent degradation domain (NODD) and C-terminal oxygen-dependent degradation domain (CODD), respectively, were incubated with PHD2 alone or with PHD2 and C16 (Fig. 3*B*). By measuring the PHD2-stimulated turnover of its ^{14}C-labeled cosubstrate 2OG to succinate, it was found that PHD2 turnover was reduced to background by C16, but not BSA (Fig. S3), at equimolar concentrations to either HIF-1α NODD or CODD. This observation suggests that C16 inhibits the binding of PHD2 to each substrate, and that C16 is not a substrate of PHD2.

To determine an IC_{50} value for the inhibition of PHD2-catalyzed HIF-1α hydroxylation by C16, the change in CODD hydroxylation with increasing levels of C16 was monitored. At a HIF-1α concentration of 50 μM, a C16 concentration of ~12 μM reduced CODD hydroxylation by 50% (Fig. 3*C*).

Next, the ability of C16 to inhibit PHD2 and stabilize HIF-1α was investigated in cells. Levels of HIF-1α in cells transfected with C16 or C6 were tested by immunoblotting. Cells treated with the generic 2OG oxygenase inhibitor and hypoxia mimic dimethyloxalylglycine (DMOG) were included as a positive control. HIF-1α was stabilized by C16 or DMOG, but not by C6 (Fig. 4*A*).

HIF-1α–induced transcription was also investigated by measuring mRNA levels of the HIF-responsive genes *VEGF* and glucose transporter 1 (*GLUT1*) by quantitative RT-PCR (qRT-PCR) (16) in cells transfected with either C16 or C6. As expected, DMOG induced transcription of both genes (Fig. 4*B*).

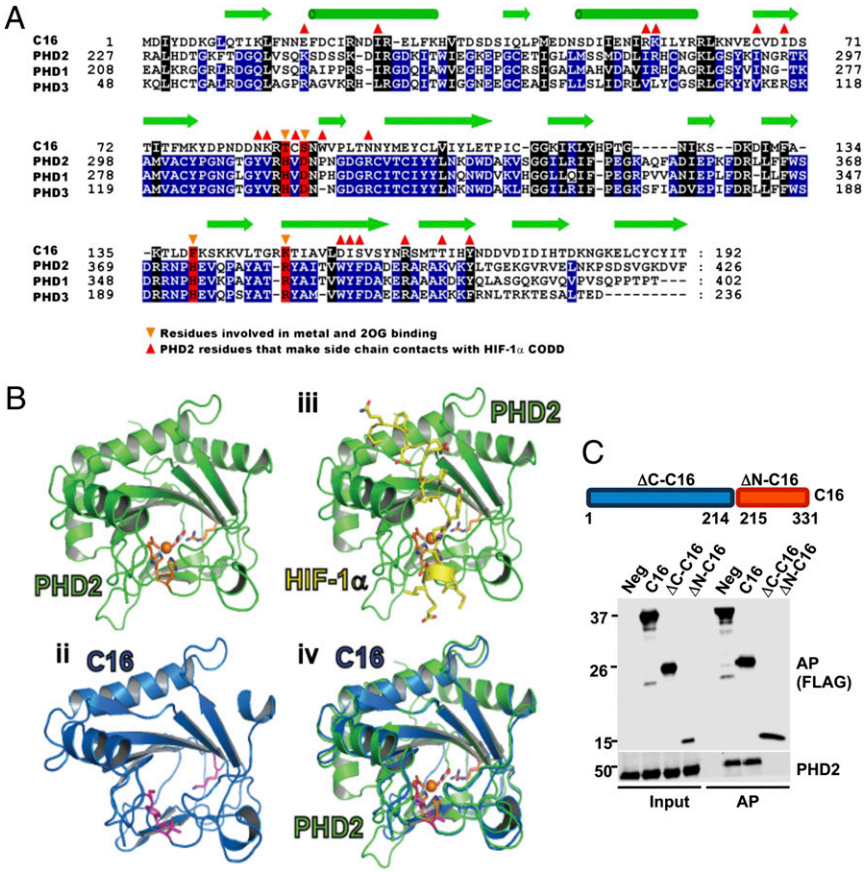

Fig. 2. The N-terminal region of C16 has a predicted PHD2-like conformation. (*A*) Protein sequence alignment of C16 amino acids 1–192 and the C-terminal regions of PHD1-3; black and blue shading indicates amino acid conservation; red shading highlights Fe(II) and 2OG coordinating residues. The predicted secondary structure of C16 is indicated by green cylinders (α-helices) or arrows (β-sheets). (*B ii*) Predicted structure of C16 residues 1–174 (in blue) based on the solved structure of $PHD2_{181–426}$ (*i*, in green; residues coordinating Fe(II) and 2OG in orange) using Modeler software. (*iii* and *iv*) PHD2 when bound to its HIF-1α CODD substrate (in yellow; *iii*) and overlayed with the predicted structure of C16 (*iv*). (*C*) Lysates from HEK293T cells transfected with full-length VACV C16, or with the N-terminal (ΔC-C16) or C-terminal (Δ*N*-C16) regions of C16 were affinity purified (AP) with streptavidin agarose. Proteins contained in whole cell lysates (Input) and in AP fractions were separated by SDS/PAGE and analyzed by immunoblotting using Abs against FLAG and PHD2. The positions of molecular mass markers are shown in kDa.

Similarly, mRNAs for both genes were up-regulated by C16, but not C6, confirming that inhibition of PHD2 by C16 is sufficient to induce HIF-1α activity (Fig. 4*B*).

HeLa cells were also transfected with C16 or C6 and a reporter plasmid in which expression of firefly luciferase is driven by the HIF-responsive element (HRE). Cells transfected with empty vector or treated with DMOG were included as negative and positive controls, respectively. Reporter gene activity was significantly higher in cells transfected with C16 than in cells transfected with C6 or with empty vector, showing that expression of C16 alone is sufficient to activate HIF-1α signaling (Fig. 4*C*).

C16 Induces HIF-1α Stabilization and Transcription of HIF-Inducible Genes During VACV Infection. Next, HIF-1α stabilization and translocation were studied in HeLa cells infected with wild-type VACV (vC16) or a mutant lacking the *C16L* gene (vΔC16; ref. 11). Immunoblotting showed stabilization of HIF-1α from 30 min postinfection (pi) with vC16, a peak at 4 h pi, and a decline thereafter. Protein C16 was also detected by 30 min pi, supporting a temporal correlation between the expression of C16 and stabilization of HIF-1α. In contrast, HIF-1α levels remained low after infection with vΔC16 (Fig. 5*B*). The translocation of HIF-1α into the nucleus was also tested by immunofluorescence. Treatment of cells with DMOG, or infection with vC16, induced HIF-1α stabilization and nuclear translocation, whereas infection with vΔC16 did not (Fig. 5*C*). Collectively, these data show that C16 is the primary VACV protein mediating HIF-1α stabilization (Fig. 5*B*). Accumulation of HIF-1α was not due to increased transcription of HIF-1α, because HIF-1α mRNA levels remained similar during infection with vC16 and vΔC16 (Fig. S4*A*); furthermore, levels of hydroxylated HIF-1α are lower in cells infected with vC16 than with vΔC16, supporting the hypothesis that C16 induces HIF-1α stabilization by preventing PHD2-mediated hydroxylation (Fig. S4*B*).

Finally, to investigate whether C16 also influences the transcription of HIF-1α–responsive genes during infection, mRNA levels of pyruvate dehydrogenase kinase (PDK) -1, GLUT-1, and VEGF (16, 26) were measured by qRT-PCR in cells infected with vC16, vΔC16, or vC16rev (a revertant with C16 reinserted into vΔC16; ref. 11). Transcription of all three genes was lower in cells infected with vΔC16 than in cells infected with viruses expressing C16. Collectively, these data show that C16 is necessary for the induction of transcription of HIF-1α–responsive genes.

Discussion

This study shows that VACV protein C16 binds to the oxygen sensing enzyme PHD2 and inhibits its hydroxylation of HIF-1α, so that HIF-1α is stabilized and its transcriptional response activated. Deletion of gene *C16L* from VACV abolished HIF-1α stabilization and prevented HIF-1α–induced transcription. In addition, ectopic expression of C16 recapitulated observations from wild-type VACV infection, showing that C16 is both necessary and sufficient to induce stabilization of HIF-1α and to activate the hypoxic response.

The interaction between C16 and PHD2 was identified using an unbiased proteomic approach and was confirmed by affinity purification in transfected and infected cells, and by interaction of recombinant protein in vitro. C16 did not bind the PHD2 isozymes PHD1 and PHD3, showing a PHD2-specific interaction. PHD1, PHD2, and PHD3 are considered to be nonredundant and are likely to contribute differently to the establishment of the cell hypoxic response (18, 19) and other roles have been suggested for each protein (17). Of these three hydroxylases, PHD2 is primarily responsible for hydroxylation of

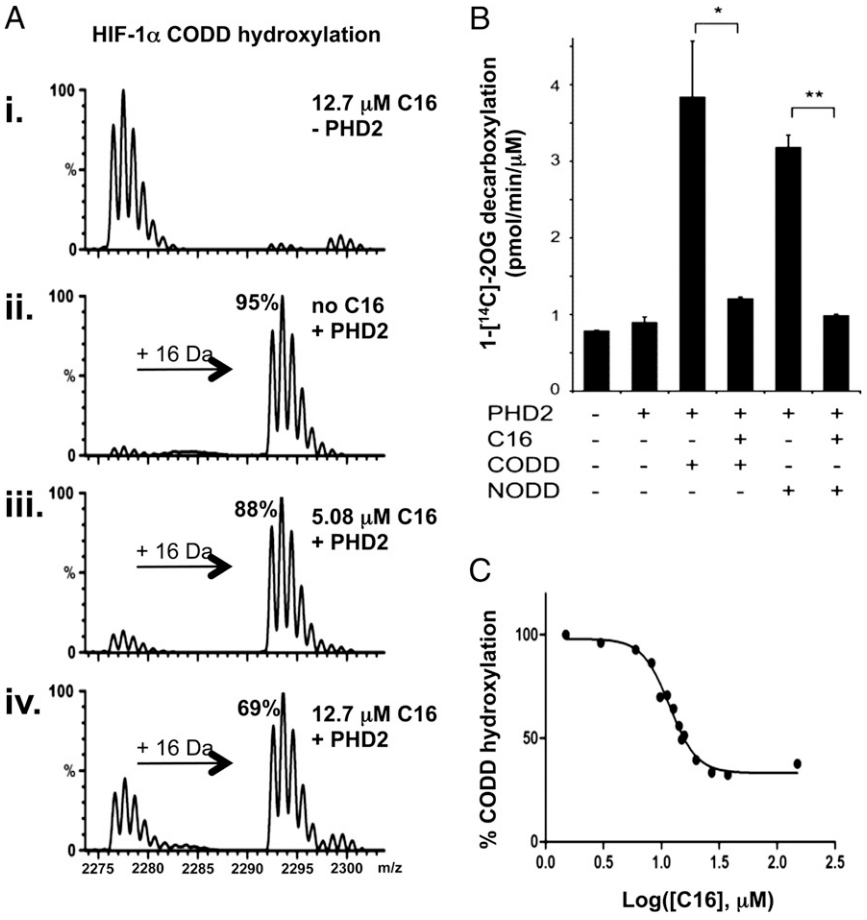

Fig. 3. C16 prevents PHD2-mediated hydroxylation of HIF-1α. (*A*) MS analysis of HIF-1α hydroxylation by PHD2 in the presence of C16. MALDI MS assays showing in vitro hydroxylation (+16 Da) of 50 μM of a HIF-1α fragment (CODD 19mer peptide) by different concentrations of C16 (12.7, 0, 5.08, and 12.7 μM in *i*, *ii*, *iii*, and *iv*, respectively) in the presence (*i*, *ii*, and *iii*) or absence (*i*) of 4 μM of PHD2 protein. (*B*) Cosubstrate turnover assay of CODD and NODD hydroxylation by PHD2 in the presence of C16. Radioactive $^{14}CO_2$ released from a 1-[^{14}C]-2OG cosubstrate upon PHD2 turnover was determined in the presence or absence of C16. C16 was used at equimolar concentration to HIF-1α CODD and NODD (50 μM); PHD2 was used at 3 μM. Error bars show SD from three technical replicates. $^{**}P < 0.01$; $^{*}P < 0.05$. (*C*) Nonlinear plot of PHD2-catalyzed HIF-1α CODD hydroxylation at varying C16 concentrations. The calculated apparent IC_{50} value for C16 protein was 11.8 ± 1 μM (95% confidence interval 10.8–12.9 μM). Assay conditions were as for *A*. Curve-fitting was performed using GraphPad Prism.

HIF-1α in normoxia (18). Like other 2OG oxygenases, it has been suggested that PHD substrate specificity might depend on regions remote from the catalytic core (24). However, our in vitro assays show that $PHD2_{181–426}$ is sufficient for C16 binding, so the N-terminal region of PHD2 is dispensable.

In vitro assays also show that as a consequence of the interaction between PHD2 and C16, the prolyl-hydroxylase activity of PHD2 on both degradation domains of HIF-1α is inhibited. These results demonstrate that this interaction is direct, because no other cellular components are required for the binding or to suppress the catalytic activity of PHD2. Direct interaction was confirmed by size-exclusion chromatography.

Interestingly, the N-terminal region of C16, which is responsible for binding PHD2, is predicted to have a similar fold to the C-terminal region of PHD2, which is responsible for the hydroxylation of HIF-1α. PHD2 has been crystallized as a homotrimer, with intermolecular contacts between the C-terminal α-helix α4 of one monomer, and the active site of the neighbor monomer (24). However, the enzyme is thought to exist as a monomer in solution, and it is therefore interesting that C16 forms a complex with PHD2 while likely assuming a PHD2-like conformation.

Despite this predicted structural similarity, the catalytic residues conserved in all animal PHDs (27) are missing in C16, suggesting not only that C16 itself is catalytically inactive, but also that it is unlikely to inhibit PHD2 by competing for Fe(II) and 2OG. Alternatively, C16 might prevent the hydroxylation of HIF-1α by sterically hindering HIF-1α binding to PHD2.

Expression of C16 was sufficient to induce stabilization of HIF-1α and up-regulation of HIF-responsive genes after transfection and viral infection, because deletion of *C16L* from VACV abolished stabilization of HIF-1α and transcription of hypoxia responsive genes. This showed that the hypoxic response is not merely an outcome of infection, but specific inhibition of PHD2 by C16.

VACV-induced stabilization of HIF-1α and induction of HIF-1α–dependent gene expression are also interesting because VACV induces a rapid shut-off of host transcription and translation (28, 29). However, stabilization of HIF-1α is induced very early after infection before the VACV-induced shutdown occurs, and reduced HIF-1α at 6 and 8 h pi might reflect the VACV shut-off as infection progresses.

Stabilization of HIF-1α after infection has been observed for other viruses, although the mechanisms and consequences of this are not entirely clear. Several oncogenic viruses stabilize HIF-1α during infection, and a link has been suggested between this and their transforming potential (30). For example, human papillomavirus (31, 32), Kaposi's sarcoma-associated herpes virus (33), Epstein–Barr virus (34–36), hepatitis B virus (37), and hepatitis C virus (38) each induce stabilization of HIF-1α. These viruses also remodel cellular metabolism by promoting aerobic glycolysis and reducing oxidative phosphorylation even in normoxic conditions, a phenomenon described as Warburg effect. In cancer cells, a reduction in mitochondrial metabolism limits production of reactive oxygen species (ROS) and accumulates metabolic intermediates that feed synthesis of nucleotides and fatty acids, features advantageous for rapidly proliferating cells (26, 30). A similar metabolic shift has been observed for other nononcogenic DNA viruses (39–41), with or without HIF-1α stabilization, suggesting that this could be important for viral replication.

In summary, this report shows that a VACV induces a hypoxic response rapidly after infection and this is mediated by protein

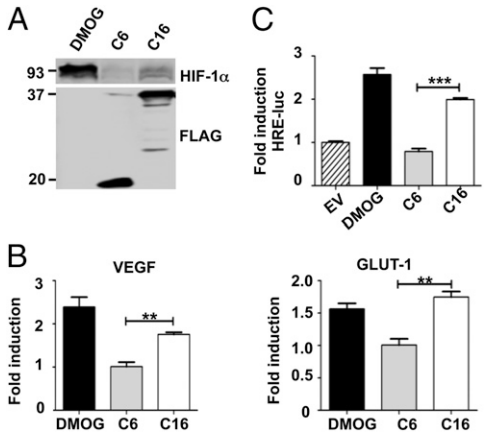

Fig. 4. C16 induces HIF-1α stabilization and hypoxic signaling. (*A*) HEK293T cells were transfected with C16 or C6 and 48 h later the levels of HIF-1α were analyzed by immunoblotting. Cells treated with DMOG were included as controls. The positions of molecular mass markers are shown in kDa. (*B*) 293T cells were transfected with C16 or C6 expression plasmids and 24 h later, the cells were lysed and RNA was extracted. Induction of *VEGF* and *GLUT-1* were measured by quantitative reverse-transcription PCR (qRT-PCR) and normalized to the housekeeping gene *HPRT*. Fold-induction is compared with C6 and was calculated using the ΔΔCT formula. The figure shows the mean ± SEM for three biological replicates. One representative of two experiments is shown. (*C*) HeLa cells were cotransfected with a firefly reporter plasmid under the control of an HIF-responsive element (HRE), a renilla luciferase transfection control and C16 or C6 expression plasmid or empty vector control (EV). After 24 h, cells were lysed and firefly and renilla activity were measured. Firefly activity was normalized to renilla luciferase activity. The fold induction is compared with EV; results are presented as mean ± SEM from four biological replicates. ***$P < 0.005$; **$P < 0.01$.

C16. The specific interaction between the N-terminal PHD2-like domain of VACV protein C16 and the C-terminal catalytic domain of PHD2 provides a precise mechanism for HIF-1α stabilization.

Materials and Methods

Plasmids. Genes were cloned in pcDNA4/TO (Invitrogen), with a C-terminal TAP tag consisting of two FLAG and two STREP epitopes (20). C16 and C4 sequences were codon optimized for mammalian cells (GeneArt).

Cell Lines and Drugs. HEK293T cells were grown in DMEM with 10% (vol/vol) FBS and penicillin and streptomycin. HEK293T cells expressing inducible C16 or PHD2 were grown in DMEM with 10% FBS with 10 μg/mL blasticidin and 100 μg/mL zeocin. Murine embryo fibroblasts (MEFs) were grown in DMEM with 15% (vol/vol) FBS. HeLa cells were grown in MEM with 10% FBS and 1× nonessential amino acids (from 100× solution, Gibco). Dimethyloxalylglycine (DMOG) and doxycycline (both Sigma) was used at 1 mM and 2 μg/mL respectively. MG132 (Calbiochem) was used at 25 μM.

Affinity Purification and Immunoprecipitation. Cells were transfected with *Trans*IT-LT1 transfection reagent (Mirus), or induced with doxycycline and then infected as indicated. Cells were lysed in lysis buffer [150 mM NaCl/20 mM Tris·HCl, pH 7.4/10 mM $CaCl_2$/0.1% Triton X-100/10% (vol/vol) glycerol and protease inhibitors (complete Mini, EDTA-free tablets, Roche)] and then incubated with Strep-Tactin beads (IBA) for 2 h. After three washes in lysis buffer, bound proteins were analyzed by SDS/PAGE and immunoblotting. For endogenous immunoprecipitations, mouse mAb anti-PHD2 antibody (Millipore) or mouse mAb anti–HIF-1α abs (BD Biosciences) was used at 1:100.

Immunoblot Analysis. For HIF-1α immunoblotting, cells were lysed in 8 M urea, 10 mM Tris·HCl (pH 6.8), 10% (vol/vol) glycerol, 1% SDS, 1 mM DTT, and protease inhibitor. Abs used were: rabbit anti-C16 (11); rabbit anti-C6 (21); mouse mAb anti-FLAG (Sigma-Aldrich); rabbit anti-PHD2 (Cell Signaling Technology); rabbit anti-PHD1 (Novus Biologicals); rabbit anti-PHD3; mouse mAb anti–HIF-1α (BD Biosciences); rabbit anti OH-HIF-1α (P564, Cell Signaling Technology); mouse mAb Ab1.1 anti-VACV protein D8 (42); and mouse mAb anti-tubulin (Upstate Biotech). Bound Ig was detected with fluorescence-conjugated goat anti-mouse or anti-rabbit and infrared technology (Licor Biotechnology).

Immunofluorescence. HeLa cells were infected at 10 pfu per cell or treated with 1 mM DMOG for 6 h and immunofluorescence was done as described (12) using anti–HIF-1α mAb (BD Biosciences, 610958).

Bioinformatic Analyses. Sequence alignments were created with Clustal and manually curated using GeneDoc. Protein structure predictions were based on the cosubstrate structure of PHD2 with HIF-1α CODD (PDB 3HQR) (25) and were prepared using Modeler 9 and visualized using PyMOL.

Quantitative Reverse Transcription PCR. Cells were transfected or infected as indicated in six-well plates. Total cellular RNA was extracted using RNEasy kit (Qiagen) and reverse transcribed with random hexamer primers according to standard methods. PCR analysis using specific primers (sequences in supplementary information) was performed with Fast SYBR Green Master Mix (Applied Biosystems) and analyzed on a ViiA 7 instrument using ViiA 7 RUO software (Applied Biosystems). The housekeeping gene

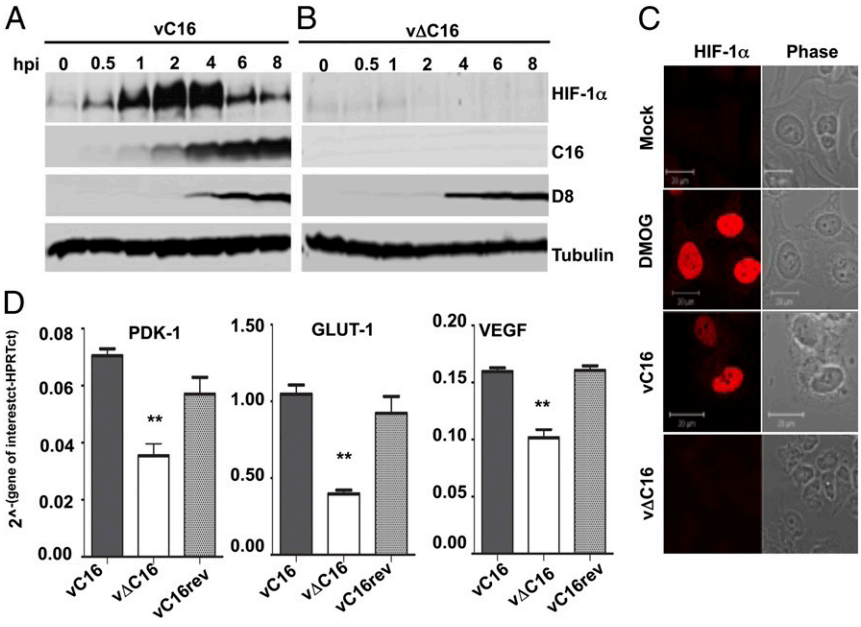

Fig. 5. Infection by VACV induces stabilization of HIF-1α and hypoxic signaling. HeLa cells were infected with vC16 (*A*) or vΔC16 (*B*) at 5 pfu per cell and, at the times indicated, cells were lysed and the levels of HIF-1α, VACV proteins C16 and D8, and tubulin were analyzed by SDS/PAGE and immunoblotting. Mock-infected cells and cells treated with DMOG were included as controls. One representative of three experiments is shown. (*C*) HeLa cells were infected with vC16 or vΔC16 at 10 pfu per cell for 6 h, and stabilization and nuclear translocation of HIF-1α were visualized by immunofluorescence. Mock-infected cells and cells treated with DMOG were included as controls. The localization of HIF-1α (red; *Left*) and a phase-contrast image (*Right*) are shown. (*D*) Deletion of *C16L* reduces transcription of HIF-responsive genes. MEFs were infected with vC16, vΔC16, or vC16rev at 10 pfu per cell and, 3 h later, cells were lysed and RNA was extracted. Induction of *GLUT-1*, *PDK-1*, and *VEGF* were measured by qRT-PCR and normalized to the housekeeping gene *HPRT*, using the formula: $2^{-(\text{Gene of interest ct}-\text{HPRTct})}$. The figure shows the mean ± SEM from three biological duplicate. **$P < 0.01$.

hypoxanthine-guanine phosphoribosyltransferase (HPRT) was analyzed in the same samples. Data were analyzed using GraphPad Prism, and *P* values were calculated using Student *t* test.

Luciferase Reporter Assay. Luciferase reporter-gene assays were performed in HeLa cells transfected with 10 ng of GL3-Renilla plasmid, 60 ng of HRE–firefly reporter plasmid (gift from Peter J. Ratcliffe, University of Oxford, Oxford, United Kingdom), and 50 ng of expression vectors or pcDNA4.0/TO empty vector control per 50,000 cells. After 24 h transfected cells were harvested in Passive Lysis Buffer (Promega) and renilla and luciferase activity were measured on a FLUOstar Omega instrument (BMG Labtech). Firefly luciferase activity was normalized against renilla luciferase activity, data were analyzed using GraphPad Prism, and *P* values were calculated using the Student *t* test.

PHD2 Hydroxylation Assay. Hydroxylation of HIF-1α peptides was analyzed using MALDI MS in the positive ion mode. Peptide samples were prepared under 2OG decarboxylation assay conditions without radioactive 2OG. Reactions were quenched with an equal volume of CH_3CN. All samples for MALDI MS analyses were mixed with α-cyano-4-hydroxy-cinnamic acid as matrix (1:1). For C16 inhibition studies of PHD2 activity, nonlinear regression analyses were performed using GraphPad Prism.

1-[^{14}C]-2OG Decarboxylation Assay. HIF-1α peptides with or without C16 protein were tested for their ability to stimulate PHD2-dependent decarboxylation of 1-[^{14}C]-labeled 2OG. Standard assay conditions comprised a total volume of 100 μL in 50 mM Tris·HCl (pH 7.5), 4 mM ascorbate, 292 μM 2OG [1.25% (wt/wt) 1-[^{14}C]], 100 μM $(NH_4)_2Fe(SO_4)_2{\cdot}6H_2O$, 0.66 mg/mL catalase ($H_2O_2$ scavenger), 4 μM enzyme and 50 μM HIF-1α peptides. Briefly, the assay was set up in three drops, one containing PHD2 (10 μL), another containing HIF-1α peptide and C16 protein (5 μL each) and the other containing reagents. Then 200 μL of hyamine hydroxide was added, the reaction tube was sealed with a rubber septum and incubated with shaking at 37 °C for 15 min and then quenched with methanol (200 μL). Reaction tubes were then kept on ice for 20 min, before the hyamine hydroxide was removed and radioactivity was counted (Beckman, LS6500). Assays were performed in triplicate. *P* values were calculated using Student *t* test (two-tailed; assuming groups have unequal variance).

ACKNOWLEDGMENTS. We thank Drs. E. Paleolog, S. Kirkiadis, N. Masson, and P. J. Ratcliffe for helpful discussions and C. J. Schofield for plasmids and reagents. C.L. was supported by a Leverhulme Trust Early Career Fellowship and a Junior Research Fellowship (JRF) from St. Edmund Hall, University of Oxford; G.L.S. was supported by a Wellcome Trust Principal Research Fellowship; N.E.P. was supported by a UK Medical Research Council doctoral studentship; and B.J.F. was supported by a JRF from Imperial College London.

1. Fenner F, Anderson DA, Arita I, Jezek Z, Ladnyi ID (1988) *Smallpox and its eradication* (World Health Organization, Geneva).
2. Moss B (2007) Poxviridae: The viruses and their replicaton. *Fields Virology*, ed Knipe DM (Lippincott Williams & Wilkins, Philadelphia), 5th Ed, Vol 2, pp 2905–2946.
3. Smith GL, Murphy BR, Moss B (1983) Construction and characterization of an infectious vaccinia virus recombinant that expresses the influenza hemagglutinin gene and induces resistance to influenza virus infection in hamsters. *Proc Natl Acad Sci USA* 80(23):7155–7159.
4. Bennink JR, Yewdell JW, Smith GL, Moss B (1986) Recognition of cloned influenza virus hemagglutinin gene products by cytotoxic T lymphocytes. *J Virol* 57(3):786–791.
5. Osman M, et al. (1999) Identification of human herpesvirus 8-specific cytotoxic T-cell responses. *J Virol* 73(7):6136–6140.
6. Moore JB, Smith GL (1992) Steroid hormone synthesis by a vaccinia enzyme: A new type of virus virulence factor. *EMBO J* 11(9):3490.
7. Reading PC, Moore JB, Smith GL (2003) Steroid hormone synthesis by vaccinia virus suppresses the inflammatory response to infection. *J Exp Med* 197(10):1269–1278.
8. Weir JP, Bajszár G, Moss B (1982) Mapping of the vaccinia virus thymidine kinase gene by marker rescue and by cell-free translation of selected mRNA. *Proc Natl Acad Sci USA* 79(4):1210–1214.
9. Hughes SJ, Johnston LH, de Carlos A, Smith GL (1991) Vaccinia virus encodes an active thymidylate kinase that complements a cdc8 mutant of Saccharomyces cerevisiae. *J Biol Chem* 266(30):20103–20109.
10. Slabaugh M, Roseman N, Davis R, Mathews C (1988) Vaccinia virus-encoded ribonucleotide reductase: Sequence conservation of the gene for the small subunit and its amplification in hydroxyurea-resistant mutants. *J Virol* 62(2):519–527.
11. Fahy AS, Clark RH, Glyde EF, Smith GL (2008) Vaccinia virus protein C16 acts intracellularly to modulate the host response and promote virulence. *J Gen Virol* 89(Pt 10):2377–2387.
12. Ember SW, Ren H, Ferguson BJ, Smith GL (2012) Vaccinia virus protein C4 inhibits NF-κB activation and promotes virus virulence. *J Gen Virol* 93(Pt 10):2098–2108.
13. Ivan M, et al. (2001) HIFalpha targeted for VHL-mediated destruction by proline hydroxylation: Implications for O2 sensing. *Science* 292(5516):464–468.
14. Jaakkola P, et al. (2001) Targeting of HIF-alpha to the von Hippel-Lindau ubiquitylation complex by O2-regulated prolyl hydroxylation. *Science* 292(5516):468–472.
15. Semenza GL (2012) Hypoxia-inducible factors in physiology and medicine. *Cell* 148(3): 399–408.
16. Schofield CJ, Ratcliffe PJ (2004) Oxygen sensing by HIF hydroxylases. *Nat Rev Mol Cell Biol* 5(5):343–354.
17. Fong GH, Takeda K (2008) Role and regulation of prolyl hydroxylase domain proteins. *Cell Death Differ* 15(4):635–641.
18. Berra E, et al. (2003) HIF prolyl-hydroxylase 2 is the key oxygen sensor setting low steady-state levels of HIF-1alpha in normoxia. *EMBO J* 22(16):4082–4090.
19. Appelhoff RJ, et al. (2004) Differential function of the prolyl hydroxylases PHD1, PHD2, and PHD3 in the regulation of hypoxia-inducible factor. *J Biol Chem* 279(37): 38458–38465.
20. Gloeckner CJ, Boldt K, Schumacher A, Roepman R, Ueffing M (2007) A novel tandem affinity purification strategy for the efficient isolation and characterisation of native protein complexes. *Proteomics* 7(23):4228–4234.
21. Unterholzner L, et al. (2011) Vaccinia virus protein C6 is a virulence factor that binds TBK-1 adaptor proteins and inhibits activation of IRF3 and IRF7. *PLoS Pathog* 7(9): e1002247.
22. Sumner RP, Ren H, Smith GL (2013) Deletion of immunomodulator C6 from vaccinia virus strain Western Reserve enhances virus immunogenicity and vaccine efficacy. *J Gen Virol* 94(Pt 5):1121–1126.
23. Sali A, Potterton L, Yuan F, van Vlijmen H, Karplus M (1995) Evaluation of comparative protein modeling by MODELLER. *Proteins* 23(3):318–326.
24. McDonough MA, et al. (2006) Cellular oxygen sensing: Crystal structure of hypoxia-inducible factor prolyl hydroxylase (PHD2). *Proc Natl Acad Sci USA* 103(26):9814–9819.
25. Chowdhury R, et al. (2009) Structural basis for binding of hypoxia-inducible factor to the oxygen-sensing prolyl hydroxylases. *Structure* 17(7):981–989.
26. Kim JW, Tchernyshyov I, Semenza GL, Dang CV (2006) HIF-1-mediated expression of pyruvate dehydrogenase kinase: A metabolic switch required for cellular adaptation to hypoxia. *Cell Metab* 3(3):177–185.
27. Loenarz C, et al. (2011) The hypoxia-inducible transcription factor pathway regulates oxygen sensing in the simplest animal, Trichoplax adhaerens. *EMBO Rep* 12(1):63–70.
28. Moss B (1968) Inhibition of HeLa cell protein synthesis by the vaccinia virion. *J Virol* 2(10):1028–1037.
29. Rubins KH, Hensley LE, Relman DA, Brown PO (2011) Stunned silence: Gene expression programs in human cells infected with monkeypox or vaccinia virus. *PLoS ONE* 6(1):e15615.
30. Noch E, Khalili K (2012) Oncogenic viruses and tumor glucose metabolism: Like kids in a candy store. *Mol Cancer Ther* 11(1):14–23.
31. Nakamura M, et al. (2009) Hypoxia-specific stabilization of HIF-1alpha by human papillomaviruses. *Virology* 387(2):442–448.
32. Tang X, et al. (2007) Overexpression of human papillomavirus type 16 oncoproteins enhances hypoxia-inducible factor 1 alpha protein accumulation and vascular endothelial growth factor expression in human cervical carcinoma cells. *Clin Cancer Res* 13(9):2568–2576.
33. Carroll PA, Kenerson HL, Yeung RS, Lagunoff M (2006) Latent Kaposi's sarcoma-associated herpesvirus infection of endothelial cells activates hypoxia-induced factors. *J Virol* 80(21):10802–10812.
34. Darekar S, et al. (2012) Epstein-Barr virus immortalization of human B-cells leads to stabilization of hypoxia-induced factor 1 alpha, congruent with the Warburg effect. *PLoS ONE* 7(7):e42072.
35. Kondo S, et al. (2006) EBV latent membrane protein 1 up-regulates hypoxia-inducible factor 1alpha through Siah1-mediated down-regulation of prolyl hydroxylases 1 and 3 in nasopharyngeal epithelial cells. *Cancer Res* 66(20):9870–9877.
36. Wakisaka N, et al. (2004) Epstein-Barr virus latent membrane protein 1 induces synthesis of hypoxia-inducible factor 1 alpha. *Mol Cell Biol* 24(12):5223–5234.
37. Yoo YG, et al. (2003) Hepatitis B virus X protein enhances transcriptional activity of hypoxia-inducible factor-1alpha through activation of mitogen-activated protein kinase pathway. *J Biol Chem* 278(40):39076–39084.
38. Nasimuzzaman M, Waris G, Mikolon D, Stupack DG, Siddiqui A (2007) Hepatitis C virus stabilizes hypoxia-inducible factor 1alpha and stimulates the synthesis of vascular endothelial growth factor. *J Virol* 81(19):10249–10257.
39. Chen IT, et al. (2011) White spot syndrome virus induces metabolic changes resembling the warburg effect in shrimp hemocytes in the early stage of infection. *J Virol* 85(24):12919–12928.
40. Abrantes JL, et al. (2012) Herpes simplex type 1 activates glycolysis through engagement of the enzyme 6-phosphofructo-1-kinase (PFK-1). *Biochim Biophys Acta* 1822(8):1198–1206.
41. McFarlane S, Nicholl MJ, Sutherland JS, Preston CM (2011) Interaction of the human cytomegalovirus particle with the host cell induces hypoxia-inducible factor 1 alpha. *Virology* 414(1):83–90.
42. Parkinson JE, Smith GL (1994) Vaccinia virus gene A36R encodes a M(r) 43-50 K protein on the surface of extracellular enveloped virus. *Virology* 204(1):376–390.